JOM, Vol. 69, No. 1, 2017
DOI: 10.1007/s11837-016-2169-6

Mechanical Anisotropy and Pressure Induced Structural Changes in Piroxicam Crystals Probed by In Situ Indentation and Raman Spectroscopy

PRAVEENA MANIMUNDA,[1,3] ERIC HINTSALA,[1] SYED ASIF,[1] and MANISH KUMAR MISHRA[2,4]

1.—Hysitron Incorporated, Minneapolis, MN 55344, USA. 2.—Department of Chemistry, McGill University, Montreal, QC H3A 0B8, Canada. 3.—e-mail: praveena.manimunda@gmail.com. 4.—e-mail: mishra_mani07@yahoo.in

The ability to correlate mechanical and chemical characterization techniques in real time is both lacking and powerful tool for gaining insights into material behavior. This is demonstrated through use of a novel nanoindentation device equipped with Raman spectroscopy to explore the deformation-induced structural changes in piroxicam crystals. Mechanical anisotropy was observed in two major faces ($0\bar{1}1$) and (011), which are correlated to changes in the interlayer interaction from in situ Raman spectra recorded during indentation. The results of this study demonstrate the considerable potential of an in situ Raman nanoindentation instrument for studying a variety of topics, including stress-induced phase transformation mechanisms, mechanochemistry, and solid state reactivity under mechanical forces that occur in molecular and pharmaceutical solids.

INTRODUCTION

High force and displacement resolution made instrumented nanoindentation a valuable tool for characterizing nanostructured materials. A desire to correlate mechanical property measurements with other characterization techniques has led to the recent popularity of in situ transmission electron microscope (TEM) and scanning electron microscope (SEM) nanoindentation for high-resolution imaging.[1–3] Not as well addressed is chemical characterization, which is equally important. For instance, the surface chemistry of the nanostructured materials plays an important role in some of the physical properties such as adhesion or wear resistance. One challenge is that there are not many tools capable of detecting chemical and mechanical property changes in real time, therefore generally, postmortem chemical analysis is performed. Development of instrumentation that can combine a surface sensitive spectroscopy technique with instrumented indentation would be powerful as it allows one to understand the physiochemical processes associated with indentation.

Raman spectroscopy is a widely-used nondestructive chemical analysis method that is capable of detecting the changes in the stress state, molecular orientation, crystallinity and phase transformation in materials.[4] The combination of high spatial resolution (~1 um) and optical microscopy makes it an ideal spectroscopy technique for in situ studies.[5–8] For example, Gerbig et al. combined confocal Raman spectroscopy with an instrumented indentation device to probe pressure induced phase transition in silicon thin films.[9–11] In the present study, a slightly modified in situ Raman and indentation methodology was adopted to probe pressure induced transformation.

In the context of industrial pharmaceutical manufacturing, the mechanical properties such as grindability and tabletability of the drug materials often used by manufacturers to determine the processing steps. The mechanical properties of molecular materials have long been studied by chemists and material engineers, although they lacked the tools to yield quantitative scientific mechanical measurements. Nevertheless, a new era has arrived with the advent of instrumented

(Published online November 9, 2016)

nanoindentation techniques. Nanoindentation is ideal for, and has been extensively used by manufactures in, determining the mechanical properties of small volume materials such as thin films and fibers. This naturally extends to the study of molecular single crystals, which are often available only in small sizes as well.[12,13] The most important role for nanoindentation in molecular solids is the establishment of structure–property correlations. In particular, fundamental insight into the effects of structural features such as crystal packing, the strength of intermolecular interactions, polymorphism, layer migration, domain coexistence, and solid state reactivity on mechanical properties such as stiffness and strength can be explored through nanoindentation studies.[12–16]

Recently, nanoindentation and post mortem Raman spectroscopy have been used to probe different polymorphs of drug materials.[17] In the pharmaceutical industry, the processing of the drug samples is a major challenge,[18,19] as the milling process can transform a crystalline starting material into an amorphous form or different polymorph.[15] In addition to this, the identification of the polymorph of the starting material is sometimes challenging. Piroxicam, which is prescribed by physicians as an anti-inflammatory drug, is an example of a drug that exhibits different polymorphs.[19,20] Intra-molecular and inter-molecular interactions, along with hydrogen bonding, gives anisotropic mechanical properties. To gain a detailed understanding of the changes in molecular interactions associated with external application of pressure, the present study used in situ Raman spectroscopy and nanoindentation. In particular, the variation of mechanical properties in the $(0\bar{1}1)$ and (011) crystallographic planes and the associated chemical changes under indentation were studied in detail.

MATERIALS AND METHODS

Large single crystals of β-form piroxicam (denoted as piroxicam) were grown in conical flasks from commercially available piroxicam (Sigma Aldrich) and were crystallized by slow evaporation of a saturated solution of methanol at room temperature. Piroxicam crystallizes in the monoclinic crystal system with the centrosymmetric space group $P2_1/c$. The single crystals, as grown in block morphology, show two major faces, (011) and $(0\bar{1}1)$ with a smooth surface suitable for the indentation experiments.

The structure of the piroxicam is shown in Fig. 1a and a schematic of the indentation-Raman device is shown in Fig. 1b. A diamond Berkovich indenter was used as the probe. A custom in situ Raman indenter (Hysitron, Inc., USA) was integrated with a free-space Raman microscope (Invia Raman Spectroscpe, Renishaw, UK). As shown in Fig. 1b, the sample and the indentation axis are aligned horizontally so that the laser probe for Raman has a free path into the contact region vertically. The indenter was equipped with a three-plate capacitive transducer, with 0.02-nm displacement noise and 2 nN force noise floors. A piezomotor based XYZ translation stage with a 3-mm travel, was used to position the sample. An ultralong working distance objective lens (Olympus NPLAN, 50×) was used to collect the Raman-scattered light from the contact zone. The source of excitation was a 785-nm diode laser with a maximum power of 200 mW. During in situ spectral acquisition, the power of the laser beam was reduced to 5 mW to avoid laser burning and the Rayleigh scattered light was blocked by using an edge filter. The combination of a dispersive spectrometer with a 1200 lines/mm grating and deep depletion chip charge coupled device detector produced 1-cm^{-1} spectral resolution.

Indentation was performed at varying normal loads from 1 mN to 20 mN on $(0\bar{1}1)$ and (011) faces of the piroxicam crystal. The arrangement of piroxicam molecules along $(0\bar{1}1)$ and (011) are shown in Fig. 1c. During the indentation on the $(0\bar{1}1)$ surface, the laser probe was focused on the contact region through the (011) face and vice versa. The Raman spectra were recorded over a 50–3400 cm^{-1} spectral range with a 10 s acquisition time. In situ SEM indentation (PI 85, Hysitron Inc USA) and ex situ imaging of the indents were performed inside a FEI VERSA 3D dual-beam FIB/SEM (FEI, Hillsboro, USA). For in situ SEM indentation experiments, 20-mN and 30-mN normal loads were applied.

RESULTS AND DISCUSSION

The variation of mechanical properties on different crystallographic directions of piroxicam crystals are shown in Fig. 2. The load–displacement curves recorded from the $(0\bar{1}1)$ and (011) faces of the piroxycam crystals are compared in Fig. 2a. The $(0\bar{1}1)$ face had a hardness of 0.82 ± 0.03 GPa and 17.16 ± 0.4 GPa reduced modulus. Whereas the (011) face had 0.64 ± 0.05 GPa hardness and modulus of 16.1 ± 0.9 GPa. Pop-in events were observed in both $(0\bar{1}1)$ and (011) load displacement curves, nevertheless, at a given load $(0\bar{1}1)$ face, they had a smaller displacement in accordance with the measured hardness. The variation of hardness and reduced modulus with normal load is shown in Fig. 2b. Up to a 5-mN load, the hardness values did not vary much with load. Yet, a small dip in hardness is observed at 5-mN load. The anisotropy in slip and hardness will be discussed further a bit later.

To gain more insight on deformation behavior, in situ SEM nanoindentation was performed, primarily for ease of location of the residual indent impressions. Figure 2c and d shows SEM micrographs of the piroxicam crystal orientation during indentation on $(0\bar{1}1)$ and (011) faces. Higher loads

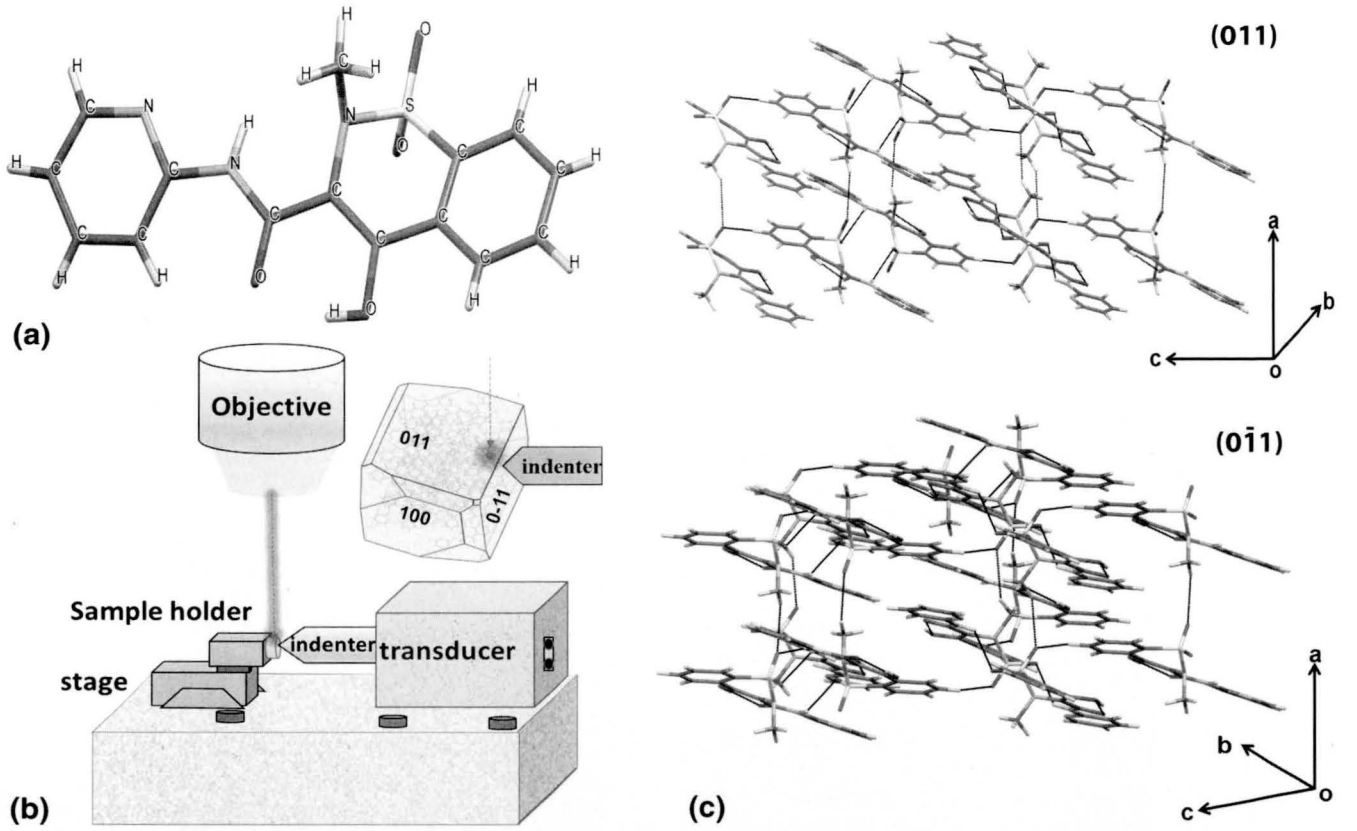

Fig. 1. (a) Structure of piroxicam. (b) Schematic shows the in situ indentation Raman device. The indentation axis and sample stage aligned horizontally, and the Raman laser was focused on to the contact region vertically. (c) Schematic shows the arrangement of piroxicam molecules along (0$\bar{1}$1) and (011).

were applied during SEM indentation (20 mN and 30 mN) to help locate the indents and image any resulting slip bands. An SEM micrograph of an indent performed on the (0$\bar{1}$1) face at 30 mN is shown in Fig. 2e. Two edges of the indent impression possessed features resembling shear bands and no visible fracturing can be observed. The indent on the (011) face had a different morphology (Fig. 2f); compared with the (0$\bar{1}$1) face, the size of the (011) indent was larger (even at a 20-mN load) with less pronounced shear bands, although some striations were observed within the indent region. The possible reason for the observed mechanical anisotropy are: (I) difference in the resolved shear stresses on the (010) planes when indenting on (0$\bar{1}$1) and (011) faces, (II) variation in interlayer interaction along [001] and [010] directions. The mechanical properties of the molecular crystals vary from one crystallographic faces to another because of structural anisotropy in terms of the packing and intermolecular interactions. Distinct variations of the plastic deformation within the same structural class occur as a result of crystal anisotropy. Previous nanoindentation study by Kiran et al. showed the mechanical anisotropy on the different faces (100) and (011) of the saccharin crystals.[21]

To understand the role of chemical interactions on the mechanical properties of the crystal, the structure of piroxicam should be revisited and discussed in greater detail. The main building block of the piroxicam crystal is a centrosymmetric dimer of piroxicam molecules connected by two N–H···O (3.055 Å) hydrogen bonds (Fig. 1c). Each molecule in the dimer interacts with neighboring dimers via six C–H···O hydrogen bonds to form infinite corrugated two-dimensional layers that are parallel to the (010) plane. The interactions between separate two-dimensional layers comes from one C–H···O hydrogen bond and one $\pi\cdots\pi$ stacking interaction. Thus, the principal slip planes are along the (010) planes, which is easy to visualize by looking at the structure in Figs. 1c and 4. There is still significant resistance to slip along the (010) planes considering the uneven surface from the corrugated structure and the previously discussed interactions with neighboring planes.

Raman spectroscopy is capable of detecting the changes in the chemical bonding or molecular orientation during indentation, potentially providing insight into bonding and structural changes during indentation. In situ Raman spectra recorded from the contact region during indentation are

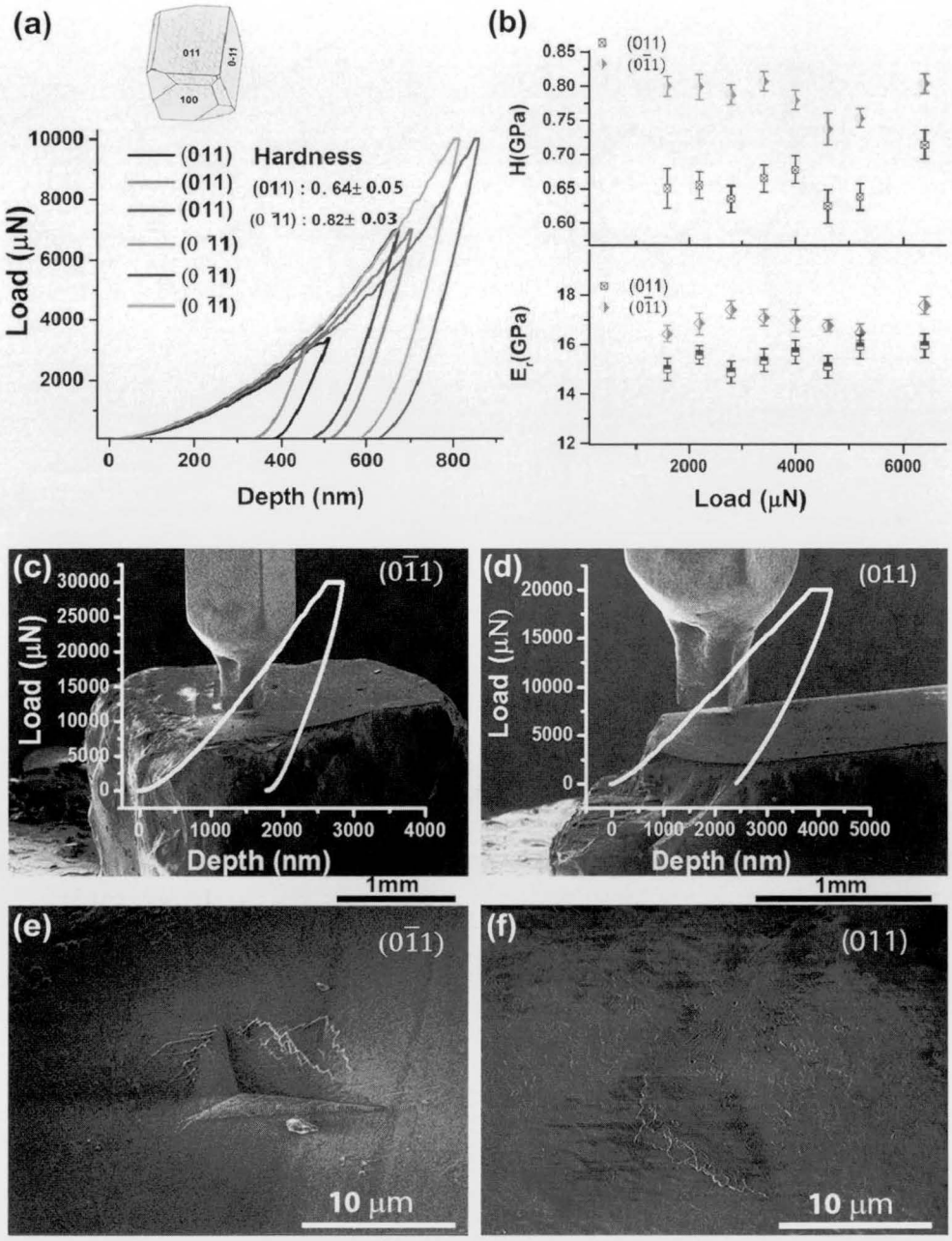

Fig. 2. Anisotropy in mechanical behavior. (a) Load displacement curves generated from (0$\bar{1}$1) and (011) faces of piroxicam crystal. (b) Variation of hardness and modulus with normal load. (c, d) Low magnification SEM micrographs shows the indentation on (0$\bar{1}$1) and (011). (e, f) Higher magnification SEM micrograph of 30-mN indent on (0$\bar{1}$1) and of 20-mN indent on (011) face. Shear band-type features were observed at the two edges of the (0$\bar{1}$1) indent.

shown in Fig. 3. First, Fig. 3a shows the in situ Raman spectra recorded during indentation on the (0$\bar{1}$1) face. In the case of piroxicam, vibrations corresponding to C–N, C=O, C–C and SO_2 (symmetric and asymmetric stretching) are expected to appear $<1850\ cm^{-1}$.[22–24] As observed in Fig. 3a, stronger bands are observed in the range of 900–1650 cm^{-1}. The vibrational modes, corresponding to C–H, N–H, and O–H stretching are in the range of 2900–3500 cm^{-1}, but the appearance of a large background made extracting qualitative information difficult, and hence 150–1800 cm^{-1} spectra is shown in Fig. 3. Four stronger bands are observed at 1334 cm^{-1} (SO_2 AS stretching), 1431 cm^{-1}, 1522 cm^{-1} and 1607 cm^{-1} (C–C vibrations). With increasing normal load, most of the spectral features remained the same; nevertheless, one major peak shift was observed during indentation, which is enhanced in Fig. 3b. Out of 22 peaks observed (Fig. 3a) the 1334 cm^{-1} band, corresponding to SO_2

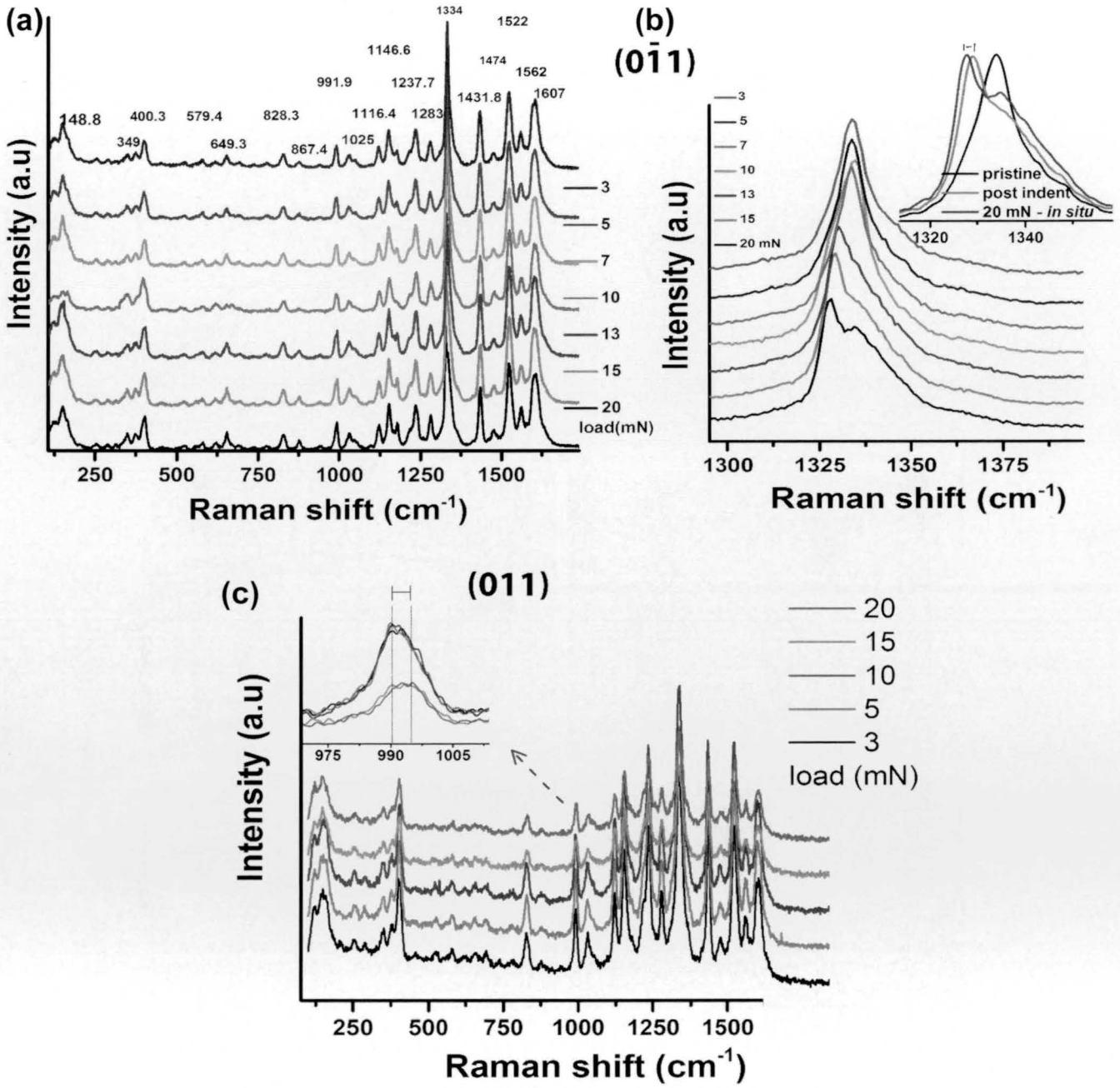

Fig. 3. In situ Raman spectra recorded from the piroxicam crystal during indentation: (a) on (0$\bar{1}$1) face and (b) zoomed in region shows variation in SO_2 stretching modes during indentation. At higher loads, the 1334-cm^{-1} peak blue shifted to 1326 cm^{-1}. Normalized in situ and ex situ 20-mN indent Raman spectra are shown in the top right corner. The spectral changes observed during in situ tests were permanent, and very small recovery is observed after pressure release. (c) In situ spectra recorded during (011) face indentation.

asymmetric stretching, blue shifted to 1326 cm^{-1} over a normal load variation from 3 mN to 20 mN (Fig. 3b). Figure 3b also shows the normalized in situ and ex situ Raman spectra. The spectral changes observed during in situ testing, did not recover completely with external pressure release. A 2 cm^{-1} recovery or red shift is observed with pressure release. Figure 3b also shows the change in shape of the 1340 cm^{-1} peak with normal load. A transition is observed at ~7 mN. Between the 5 mN and 7 mN load range, hardness values showed small dip. However, it is hard to say the drop in hardness is related to the molecular rearrangement. With 20-mN indent Raman spectra retaining modified spectral features after pressure release; it is believed that at higher loads, the spectral changes reflect the effect of shear during slip and at lower loads changes arising solely from normal stress.

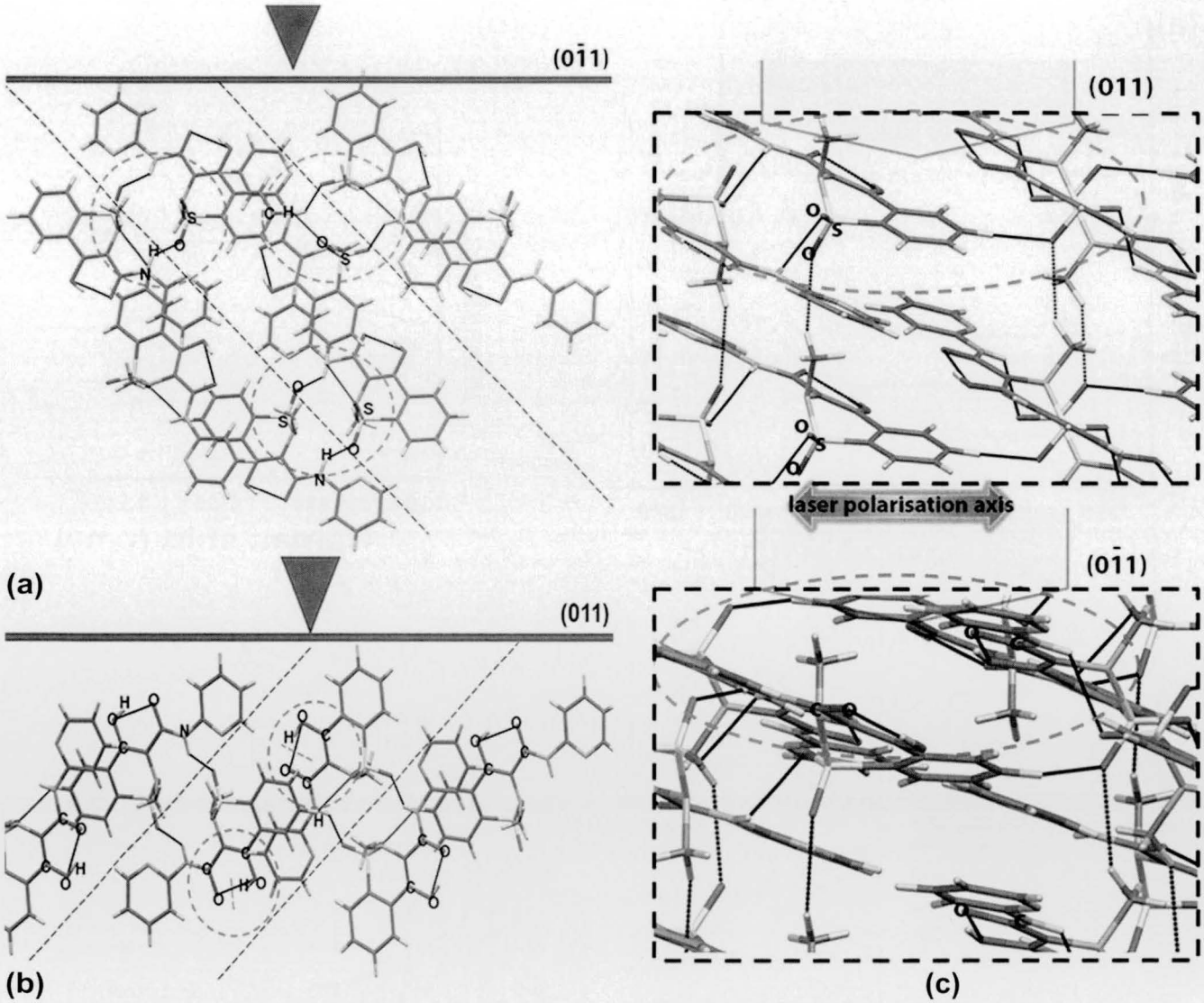

Fig. 4. (a, b) Schematic shows the orientation of the molecular chains along the indentation axis. Dotted red circles show the possible bonds affected during indentation. On (0$\bar{1}$1) surface, Raman spectra detected variation in SO_2 stretching modes, whereas indentation on (011) surface induced C–O vibrational mode changes. (c) High-magnification image shows the molecular orientation along (0$\bar{1}$1) and (011).

When indentation was done on the (011) plane, the in situ Raman spectra did not show a shift in SO_2 stretching modes, instead a small peak shift was observed at 990 cm^{-1} which corresponded to C–O stretching. At higher loads (15 mN and 20 mN), the 990 cm^{-1} band shifted to 995 cm^{-1}; this red shift in the C–O stretching vibration indicates a break in O–H···O intramolecular interaction during indentation.

For reference, the alignment of molecular chains with respect to indentation axis and (011), (0$\bar{1}$1) planes are shown in Fig. 4a and b. The dotted red circle shows the location of SO_2 and C–O molecules. Any movement of the adjacent molecular layers during indentation, will result in a strain on the SO_2 molecule. As shown in Fig. 4a, the hydrogen bond is formed between the oxygen of the SO_2 molecule and the hydrogen from the adjacent layer N–H group. The blue shift of the SO_2 stretching mode (Fig. 3b) means additional energy to stretch the sulfur and oxygen bond. The interlayer interaction may alter during compaction or slip but with one vibrational mode change (Fig. 3), it is hard to identify the actual mechanism.

Lower hardness on the (011) surface (Fig. 2) indicates easy slip along (010) during indentation. A change in SO_2 vibrational modes is expected during slip. Nevertheless, Raman spectra in Fig. 3c showed no changes in SO_2 vibrational modes; instead, a red shift in C–O stretching modes was observed. The only possible explanation is the direction of Raman measurement. With a laser beam focused on the contact region from the sides, which is through the (0$\bar{1}$1) surface when indenting on the (011) face, only bonds that are aligned parallel to the (0$\bar{1}$1) surface are expected show a

difference in spectra. The polarization axis of the Raman laser was parallel to the surface and normal to the indentation axis (shown in Fig. 4c). It is reasonable to conclude that the deformation resulted in a different bonding rearrangement for $(0\bar{1}1)$ and (011): An intralayer interaction modification (C–H···O interactions) was observed for (011) as compared with an interlayer interaction modification observed in the case of $(0\bar{1}1)$. The observed mechanical anisotropy is not solely related to the alignment of crystal planes; instead the interlayer chemical interactions also contributed to enhancing the hardness of the $(0\bar{1}1)$ surface. The results demonstrate the capability of the in situ Raman indenter to collect the chemical as well as the mechanical information in real time.

CONCLUSION

A novel indentation method was adopted to study the chemical changes associated with indentation. In situ indentation and Raman measurements provided useful insight into the mechanical anisotropy and associated structural changes in piroxicam. Specifically, the (011) face had lower hardness than did the $(0\bar{1}1)$ face, which correlated to in situ Raman spectra. The changes in SO_2 vibrational modes during indentation on the $(0\bar{1}1)$ face and C–O stretching modes during indentation on the (011) planes suggest variation in interlayer and intralayer interactions. Different interlayer interactions resulted in higher hardness for the $(0\bar{1}1)$ surface.

ACKNOWLEDGEMENTS

The authors would like to thank Prof. Gautam R. Desiraju and Dr. M.S Bobji from Indian Institute of Science Bangalore, for providing laboratory felicities.

REFERENCES

1. J.T.M. De Hosson, W.A. Soer, A.M. Minor, Z. Shan, E.A. Stach, and S.A. Asif, *J. Mater. Sci.* 41, 7704 (2006).
2. A.M. Minor, S.A. Asif, Z. Shan, E.A. Stach, E. Cyrankowski, T.J. Wyrobek, and O.L. Warren, *Nat. Mater.* 5, 697 (2006).
3. B.N. Jaya and V. Jayaram, *JOM* 68, 94 (2016).
4. I. DeWolf, *Semicond. Sci. Technol.* 11, 139 (1996).
5. D.E. Diaz-Droguett, R. El Far, V.M. Fuenzalida, and A.L. Cabrera, *Mater. Chem. Phys.* 134, 631 (2012).
6. T.W. Scharf and I.L. Singer, *Tribol. Lett.* 14, 3 (2003).
7. V.V. Poborchii, A.V. Kolobov, and K. Tanaka, *Appl. Phys. Lett.* 72, 1167 (1998).
8. F.I. Allen, E. Kim, N.C. Andresen, C.P. Grigoropoulos, and A.M. Minor, *Ultramicroscopy* (2016). doi:10.1016/j.ultramic.2016.06.011.
9. Y.B. Gerbig, C.A. Michaels, A.M. Forster, J.W. Hettenhouser, and W.E. Byrd, *Rev. Sci. Instrum.* 83, 125106 (2012).
10. Y.B. Gerbig, S.J. Stranick, and R.F. Cook, *Phys. Rev. B Condens. Matter Mater. Phys.* 83, 1 (2011).
11. Y.B. Gerbig, C.A. Michaels, A.M. Forster, and R.F. Cook, *Phys. Rev. B - Condens. Matter Mater. Phys.* 85, 104102 (2012).
12. S. Varughese, M.S.R.N. Kiran, U. Ramamurty, and G.R. Desiraju, *Angew. Chem. Int. Ed. Engl.* 52, 2701 (2013).
13. U. Ramamurty and J. Jang, *Cryst. Eng. Comm.* 16, 12 (2014).
14. S. Chattoraj, L. Shi, M. Chen, A. Alhalaweh, S. Velaga, and C.C. Sun, *Cryst. Growth Des.* 14, 3864 (2014).
15. M.K. Mishra, S. Varughese, U. Ramamurty, and G.R. Desiraju, *J. Am. Chem. Soc.* 135, 8121 (2013).
16. M.K. Mishra, U. Ramamurty, and G.R. Desiraju, *Curr. Opin. Solid State Mater. Sci.* (2016). doi:10.1016/j.cossms.2016.05.011.
17. D. Olusanmi, K.J. Roberts, M. Ghadiri, and Y. Ding, *Int. J. Pharm.* 411, 49 (2011).
18. N.S. Trasi, and S.R. Byrn, *AAPS Pharm. Sci. Tech.* 13, 772 (2012).
19. K. Naelapää, J.P. Boetker, P. Veski, J. Rantanen, T. Rades, and K. Kogermann, *Int. J. Pharm.* 429, 69 (2012).
20. W. Fortunato de Carvalho Rocha, G.P. Sabin, P.H. Marco, and R.J. Poppi, *Chemom. Intell. Lab. Syst.* 106, 198 (2011).
21. M.S.R.N. Kiran, S. Varughese, C.M. Reddy, U. Ramamurty, and G.R. Desiraju, *Cryst. Growth Des.* 10, 4650 (2010).
22. S. Suresh, S. Gunasekaran, and S. Srinivasan, *Spectrochim. Acta - Part A Mol. Biomol. Spectrosc.* 138, 447 (2015).
23. A. Lust, C.J. Strachan, P. Veski, J. Aaltonen, J. Heinämäki, J. Yliruusi, and K. Kogermann, *Int. J. Pharm.* 486, 306 (2015).
24. A. Bertoluzza, M. Rossi, P. Taddei, E. Redenti, M. Zanol, and P. Ventura, *J. Mol. Struct.* 480, 535 (1999).